


## Determination of ice production in a natural river: a case study in the Inner Mongolia Reach of the Yellow River

Zhixing Hou <sup>a</sup>, Jun Wang<sup>a</sup>, Jueyi Sui<sup>b,\*</sup>, Baosen Zhang<sup>c</sup> and Fangxiu Zhang<sup>c</sup>

<sup>a</sup> College of Civil and Hydraulic Engineering, Hefei University of Technology, Hefei, China

<sup>b</sup> School of Engineering, University of Northern British Columbia, Prince George, Canada

<sup>c</sup> Yellow River Water Conservancy Research Institute, Zhengzhou, Henan, China

\*Corresponding author. E-mail: jueyi.sui@unbc.ca

 ZH, 0000-0002-7134-7373

### ABSTRACT

In the present study, ice production in a natural river reach has been studied by means of the thermodynamic theory regarding the heat flux between ice, air, riverbed, and water. The heat transfer coefficient and equivalent total heat flux were determined for different periods during winter. The characteristics of variation and distribution of ice production in the Inner Mongolia Reach of the Yellow River (IMRYR) were studied in combination with the change of heat flux. A model for describing the temporal-spatial variation of ice production for the IMRYR has been developed. The ice production process of the IMRYR from 2017 to 2021 was simulated using the proposed model, and the simulation results were in good agreement with those of the measurements. Results of the analysis showed that when the total ice production in the Bayangaole gauging station reaches  $3.18 \times 10^7 \text{ m}^3$ , a freeze-up process in this river reach is likely to occur. The influence degree of each variable on the ice production was in the following descending order: water surface area, air temperature, radiation, and flow. Particularly, a change of 20% of the water surface area will lead to a 11.48% change in the final calculated result of ice production.

**Key words:** heat flux, ice production, Inner Mongolia Reach of the Yellow River, thermodynamics

### HIGHLIGHTS

- Ice production in Inner Mongolia Reach of the Yellow River: At present, there are some related studies on the variation characteristics of ice situation and flow in the Inner Mongolia Reach of the Yellow River, but there is hardly any study regarding ice production in a natural river.
- Thermodynamics: The water body heat exchange process and heat flux components of each part during winter were analyzed.

## 1. INTRODUCTION

During winter, a lot of ice appears in rivers in cold regions produced through the heat exchange process. Once an ice jam or ice dam is formed in the river, the flow capacity of the river is reduced. Consequently, the water level will be increased and the flow velocity under an ice jam may increase. It may cause an ice flood (Sui *et al.* 2002, 2005, 2006) and dramatical deformation of a riverbed under an ice jam (Sui *et al.* 2000). The Yellow River is one of the rivers with the most frequent ice floods in China. The main ice flood disasters are concentrated in the northernmost Inner Mongolia Reach and the downstream Hequ Reach of the Yellow River (Sui *et al.* 2002, 2005, 2006, 2007, 2008). According to incomplete statistical results from 1990 to 2019, more than 30 ice jam/ice dam events occurred in the Inner Mongolia Reach of the Yellow River (IMRYR) (Zhao *et al.* 2020).

Sufficient ice on the water surface is an essential condition for the formation of an ice jam or ice dam. When the ice discharge rate from upstream is greater than the ice transport capacity of the river reach, ice floes and frazil ice particles easily accumulate under an ice cover and form an ice jam or ice dam. The speed of the development of an ice cover or ice jam is related to the amount of ice production (Lees *et al.* 2021). Thus, the flow cross-sectional area decreases, and ultimately it leads to a decrease in the flow capacity, and an increase in the water level during an ice-jammed period. This will result in an increase in the ice jam thickness (Sui *et al.* 2002, 2005, 2008). The calculation results of ice production can provide support

This is an Open Access article distributed under the terms of the Creative Commons Attribution Licence (CC BY 4.0), which permits copying, adaptation and redistribution, provided the original work is properly cited (<http://creativecommons.org/licenses/by/4.0/>).

and guarantee for predicting the occurrence of an ice jam and the relationship between the flow and water level in a river, which has great importance for disaster prevention and mitigation (Wang *et al.* 2007, 2021).

At present, there are two typical methods for estimating ice production in a river. The first method for estimating ice production is to use the observed or calculated area of floating ice on the water surface multiplied by ice thickness to obtain the volume of ice production (Comiso *et al.* 2011). The second method for estimating ice production is to simulate the heat exchange process by establishing a thermodynamic model and calculate the volume of ice production (Cheng *et al.* 2017). The heat budget has an important influence on the river ice production in cold regions, and it is also an important part of developing a model for determining the ice production. The evolution of river ice along a river reach is influenced by the heat exchange process among the atmosphere, ice cover, flowing water in the river and riverbed, which is a key factor affecting and determining the change of water temperature and ice production (Maykut 1982; Tuo 2018). Untersteiner (1964) and Maykut & Untersteiner (1971) have been carrying out research work regarding the ice thermodynamics and modeling. Ashton (1985) summarized the heat exchange equation between the water surface and the atmosphere and between the ice cover and the atmosphere when studying the mechanism of ice cover melting. By analyzing the influence of heat budget on the temperature of an ice cover, Ashton revealed the melting process during the break-up period. Shen & Chang (1984) considered the heat exchange of the whole system at the interface of air-ice body, water surface, and riverbed, and proposed a thermodynamic model to simulate the generation and dissipation of river ice in a natural river. Using field observation data, based on other researchers' models regarding solar radiation, long-wave radiation, evaporation, and convection, Yang (2021) developed a nonlinear thermodynamic model for heat flux in rivers, lakes, and the atmosphere. However, it is not easy to obtain necessarily meteorological data for calculating the heat exchange process by using the above-mentioned nonlinear thermodynamic model. The linear thermodynamic model is normally used to study river ice hydraulics due to its advantages of simple calculation and relatively fewer requirements on meteorological data. By analyzing the heat loss between water and the atmosphere, Paily *et al.* (1974) classified different linear thermodynamic models into three categories and proposed the heat transfer coefficient in linear thermodynamic models. For linear thermodynamic models, a correct selection of the heat transfer coefficient at the ice interface is often the key factor for assessing the melting process of an ice cover (Sarraf & Zhang 1996). Marsh & Prowse (1987) compared four different methods for calculating the heat transfer coefficient and claimed that the heat transfer coefficient calculated by the Colburn analogy method was more accurate and more suitable for determining the heat flux under an ice cover. At present, most thermodynamic models only consider the influence of heat flux between the atmosphere and water on the generation and dissipation of river ice. However, the heat transfer process of ice-water interface is often ignored or considered with simple parameterized methods. When there is an ice cover on the river surface, the ice cover separates the water from the atmosphere, and the heat exchange process mediated by the ice cover is clearly different from the heat exchange between the atmosphere and water. The heat transfer process at the ice-water interface affects the ice thickness and the water temperature under the ice cover, and the adoption of an inappropriate ice-water heat flux value will affect the accuracy of the simulation of ice generation and extinction process (Benson *et al.* 2012). Li *et al.* (2016) studied the heat transfer process between the water body and the ice cover and established a linear relationship between the ice-water heat transfer coefficient and flow discharge of water under the ice cover based on experimental data in a flume. Conceptually, the heat exchange phenomenon is not an independent process but an interactive process. A complete coupled model is required for simulation of this process (Launiainen & Cheng .1998). The heat exchange between the water body and the frozen riverbanks and riverbed is also an important factor affecting the ice production in a river. The heat exchange in rivers where water temperature varies greatly from day to night should not be ignored (Mao & Chen 1999). Considering the effect of the heat flux between the ice cover and the water body and between the riverbed/riverbanks and the water body on the production of river ice, to improve the accuracy in calculation of ice production, the Colburn analogy method is coupled with the principle for solid plate heat transfer and thermodynamic model.

To date, some studies have been conducted to assess the characteristics of the ice regimen and flow in the IMRYR. However, only few studies have been carried out to study the ice production, since the amount of ice production depends on the heat exchange process which is very complicated and closely related to air temperature, meteorology, flow, and other factors. To study the features of variation of ice production in the IMRYR, the water body heat exchange process and heat flux components at each hydrological station during winter were analyzed. Then, the ice production model has been established and the features of variation in ice production have been studied.

## 2. STUDY RIVER REACH AND DATA

### 2.1. The research area

The Inner Mongolia Reach is located in the northernmost region of the Yellow River. The distance from the upstream Dengkou gauging station to the downstream Toudaoguai gauging station is 823 km long, as shown in Figure 1. The IMRYR is between 39°–41° north latitude and 106°–112° east longitude. Upstream of the Dengkou gauging station, the Yellow River is narrow with a large hydraulic slope. Then, the Yellow River enters the Houtao Plateau of the Inner Mongolia autonomous region and becomes wide. The IMRYR becomes meandering and flows from west to east. The lower section of the IMRYR is narrower than the upstream section. Due to its unique geographical feature and hydrometeorological conditions, river ice flooding happens nearly every year in the IMRYR. In the region where the IMRYR is located, the temperate continental climate prevails. Thus, the winter is cold and long with the lowest air temperature of  $-35^{\circ}\text{C}$ . The ice-covered period lasts over 4 months. Upstream of the IMRYR, the Yellow River flows from low latitude to high latitude, namely from the relatively warm region to the region with lower air temperature. With the decrease in air temperature along this reach, which has a large hydraulic slope, a vast amount of frazil ice is produced in the IMRYR during winter. These frazil ice particles form a lot of ice pans and some sections of the IMRYR gradually freeze-up in November every year. Some sections of the IMRYR are kept as open flow due to high flow velocity. During the winter period, after some sections of the IMRYR are covered by the ice cover, frazil ice and ice pans are generated in the upstream section, and open flow sections are entrained by the flowing water and submerged under the ice cover. Consequently, some ice jams form in the IMRYR every year. Since part of the IMRYR flows in the Houtao Plateau, the ice storage capacity in the channel is low. On the other hand, due to the effect of ice jams in the IMRYR, the increment of channel water storage is large which leads to an increase in the water level. Thus, flooding caused by ice jams in the IMRYR happens very often and lasts longer, especially during the periods of river freeze-up and break-up.

### 2.2. Data

To date, during the ice-covered period along this river reach, long-term systematic observations along the entire IMRYR have not been conducted for collecting data regarding wind speed, solar radiation, atmospheric pressure, and other data. In the present study, some hydrological and meteorological data are available at the following four gauging stations along the IMRYR: Bayangaole, Sanhuhekou, Baotou, and Toudaoguai, as shown in Figure 1. These gauging stations are maintained by the Yellow River Water Conservancy Commission. The following hydrological and meteorological data during a period from 2017 to 2020 have been collected from these four gauging stations: air temperature ( $T_a$ ), water temperature ( $T_w$ ), wind speed ( $V_6$ ), flow discharge ( $Q_w$ ), flow velocity ( $V$ ), and ice thickness ( $h_i$ ), with the data accuracy  $0.1^{\circ}\text{C}$ ,  $0.1\text{ m/s}$ ,  $1\text{ m}^3/\text{s}$ ,  $0.1\text{ m/s}$ , and  $0.01\text{ m}$ , respectively. Data for river cross-sections and profile along the river reach from the upstream Bayangaole station to the downstream Toudaoguai station measured in 2012 have also been collected.

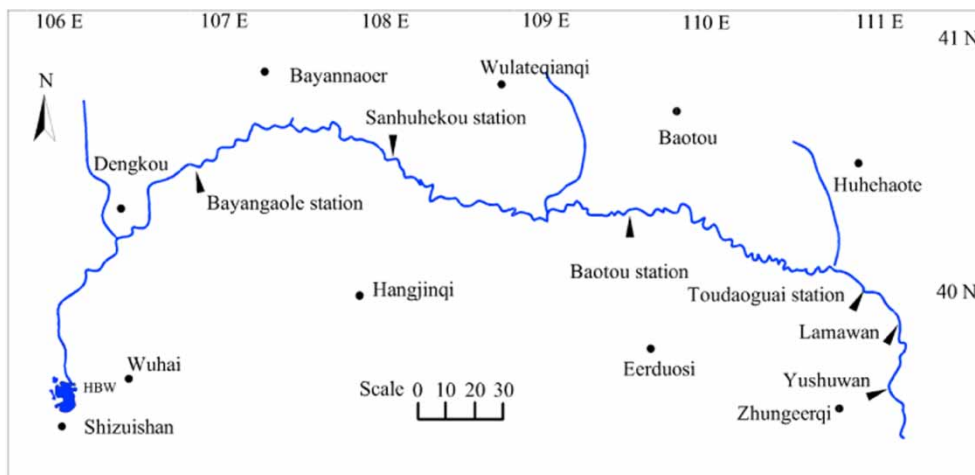


**Figure 1** | Geographical location and gauging stations in the IMRYR.

### 3. METHODOLOGY

Ice production in a river is mainly affected by the net heat flux per unit area of the river surface. The heat budget along a river reach consists of heat exchange between water and the atmosphere, heat exchange between water and riverbed, heat caused by friction between the water body and riverbed, heat flux of snow falling on the water surface, local heat flowing into the river, etc. (Shen & Ruggles 2010). When the heat transferred from local inflows such as tributaries or groundwater is small along a river reach, the influence of the heat from local inflows on the heat budget along a river reach can be ignored. The heat generated by friction between the water body and riverbed along a short reach can be also ignored. In this paper, to study ice production along the IMRYR, only the flux of heat exchange between ice, air, riverbed, and water body is considered.

The process of ice accumulation in the IMRYR can be divided into the following three stages: the ice floating period, the river freeze-up period, and the river break-up period. During the ice floating period, the water surface normally loses heat and produces frazil ice particles. Frazil ice particles emerge to the water surface. A vast amount of frazil particles collide and gradually form a lot of ice pans floating on the water surface. With the increase in the coverage rate of the water surface by ice pans, the flow velocity of the water surface decreases. If the air temperature is low enough, part of the water surface becomes frozen. As a consequence, if the flow velocity is not high enough, an ice cover will develop toward the upstream of this river reach, namely the river freeze-up period. The break-up period is a period when the ice cover on the water surface becomes broken up and melts. The river break-up process normally happens in the spring season, although it often happens during an ice-covered period due to high flow velocity with high energy.

During the ice floating period, ice covers start to grow along riverbanks or regions with the low flow velocity. The presence of the ice cover on the water surface separates the flowing water body from the atmosphere and reduces the energy exchange between the water body and the atmosphere. Thus, the heat exchange between the water body and the atmosphere needs to be carried out through the ice cover (Smits *et al.* 2021). Therefore, the heat budget due to heat exchanges in the presence of an ice cover on the water surface (partially covered along riverbanks) is the most complicated issue during the river freeze-up period. During the river freeze-up period, three heat exchange processes should be considered simultaneously, namely the heat exchanges between the atmosphere and the water body, between the ice cover and the water body, and between the water body and riverbed (including riverbanks).

Combining the heat flux of these three processes—heat exchange between the atmosphere and water, between the ice cover and water, and between water and riverbed—the equivalent total heat flux of water in river reach can be expressed as the following:

$$\phi^* = \frac{\phi_{wa}^*(B - b) + \phi_{wi}^*b + \phi_d^*\chi}{\chi + B} \quad (1)$$

where  $\phi^*$  is the net heat flux per unit length of the river;  $B$  is the river width;  $b$  is the width of the ice cover.  $\chi$  is the wetted perimeter of the riverbed;  $\phi_{wa}^*$  is the heat flux due to the heat exchange between the atmosphere and the water body;  $\phi_{wi}^*$  is the heat flux due to the heat exchange between the ice cover and the water body;  $\phi_d^*$  is the equivalent heat flux due to the heat exchange between the riverbed and the water body.

Due to the partial absence of the ice cover on the water surface, as shown in Figure 2, the heat budget during the ice floating period and river break-up period can be considered as the heat exchange between the atmosphere and the water body, as well as heat exchange between the riverbed and the water body, by considering the width of the ice cover  $b = 0$ , as shown in Figure 2.

To determine the heat flux between the atmosphere and the water body, between the ice cover and the water body, as well as between the riverbed and the water body, the following methods are used, respectively.

#### 3.1. Heat flux between the atmosphere and the water body

Current studies on the heat exchange process between the atmosphere and the water body show that the heat exchange is affected by climate and water temperature, including evaporation, convective heat transfer, long-wave solar radiation, short wave solar radiation, and so on. Therefore, heat flux due to heat exchange between the atmosphere and the water body can be expressed as:

$$\phi_{wa}^* = \phi_{Le} + \phi_{Lc} + \phi_b + \phi_r \quad (2)$$

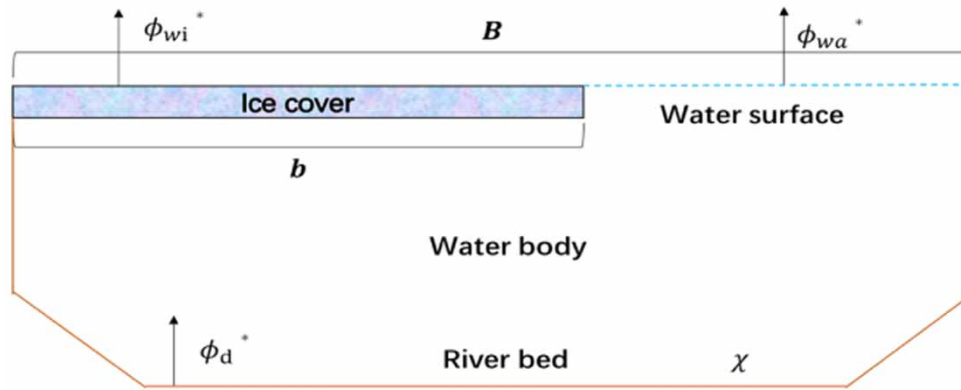


**Figure 2** | The heat budget diagram.

where  $\phi_{wa}^*$  is the heat flux due to heat exchange between the atmosphere and the water body;  $\phi_{Le}$  is the heat flux caused by evaporation;  $\phi_{LC}$  is the heat flux caused by convection;  $\phi_b$  is the heat flux caused by solar long-wave radiation;  $\phi_r$  is the heat flux caused by shortwave radiation.

Heat flux due to evaporation can be estimated by the Russian winter formula (Freysteinnsson 1970):

$$\phi_{Le} = (1.56k_e + 0.56V_6)(e_w - e_a) \quad (3)$$

where  $k_e$  is the convective influence coefficient,  $k_e = 0.926 + 0.04(T_w - T_a)$ ;  $T_w$  is the water temperature;  $T_a$  is the air temperature;  $V_6$  is the wind speed 6 m above the water surface;  $e_w$  is the saturated vapor pressure of water, which can be calculated by the Goff–Gratch formula in the reference (Bull 1920); and  $e_a$  is the saturated vapor pressure of air.

Heat flux caused by the convection process is greatly affected by the temperature difference (Freysteinnsson 1970). The heat flux caused by the convection process is estimated by the following formula (Ashton 1986):

$$\phi_{LC} = [6.04 + 2.95V_{1.5} + 0.263(T_w - T_a)](1 - R_h)e_a \quad (4)$$

where  $V_{1.5}$  is the wind speed 1.5 m above the water surface;  $R_h$  is the relative humidity in the air.

The variation of cloud coverage in the sky can easily affect the results of calculated radiation. Also as reported by the researcher, there is often an obvious error in the estimation of long-wave radiation in rivers. There is a variety of literature on the calculation of long-wave radiation, which is far beyond the scope of this study. To calculate the atmospheric long-wave radiation, the calculation method proposed by Bull (1920) is used. Based on Stefan–Boltzmann’s law, the heat flux caused by the long-wave radiation can be expressed as:

$$\phi_b = 0.97\sigma[T_w^4 - \varepsilon_a(1 + kC^2)T_a^4] \quad (5)$$

where  $\sigma$  is the Stefan–Boltzmann constant;  $\varepsilon_a$  is the atmospheric emissivity of sunny days;  $k$  is the coefficient that can be assumed as 0.17 (Ashton 1986).  $C$  is the cloud coverage and the value ranges from 0 to 1.

The heat flux caused by shortwave solar radiation is calculated by the following formula which is a function of the solar zenith angle and water vapor pressure:

$$\phi_r = \frac{Scos^2Z}{[(\cos Z + 2.7) \times e_w \times 10^{-3} + 1.085 \cos Z + 0.1]}(1 - 0.52C) \quad (6)$$

where  $S$  is the solar constant and  $Z$  is the local solar zenith angle.

### 3.2 Heat flux between the ice cover and the water body

Unlike the heat exchange between the atmosphere and the water body, the presence of an ice cover somehow prevents the heat exchange between the air and the water body. Ice cover thickness affects heat transfer between an ice cover and the water body. The top layer of an ice cover exchanges heat with the atmosphere, and the bottom part of an ice cover exchanges heat with the water body. The heat flux due to the exchange between the ice cover and the water body is relatively continuous and stable. The balance of heat flux at the bottom of the ice cover can be expressed as:

$$\phi_c + \phi_f + \phi_{wi}^* = 0 \quad (7)$$

where  $\phi_c$  is the heat flux generated by heat conduction in the ice cover;  $\phi_f$  is the latent heat flux generated by an interfacial phase transition between the ice cover and the water body;  $\phi_{wi}^*$  is the heat flux between the ice cover and the water body.

Determining the value of heat transfer coefficient is the main step in studying the heat exchange between the ice cover and the water body. The Colburn analogy method is often used to calculate the heat transfer coefficient for the water body under an ice-covered flow condition. The heat transfer coefficient  $h_{wi}$  can be calculated using the Colburn analogy method as follows,

$$h_{wi} = S_t C_v V \quad (8)$$

where  $C_v$  is the specific heat capacity;  $V$  is the flow velocity,  $S_t$  is the Stanton number which is a dimensionless parameter representing heat transfer in convection.

The heat flux between the ice cover and the water body can be expressed as:

$$\phi_{wi}^* = h_{wi}(T_s - T_w) \quad (9)$$

where  $T_s$  is the temperature of the under surface of the ice cover,  $T_w$  is the temperature of the water body.

The heat loss between the ice cover and the water body results in the decrease in the temperature of the water body, and thus freeze-up process of the water surface, as well as the thickening process of the ice cover provided the temperature is low enough. The ice production in the river will also be affected during the process of convective heat transfer and heat conduction.

### 3.3. Heat flux between the riverbed and the water body

The change in air temperature can directly affect the change of ground temperature. However, the fluctuation frequency and amplitude of the process of ground temperature change are quite different from that of the air temperature change process. The process of ground temperature change has the characteristics of slow change with a small fluctuation amplitude, which is embodied in the gentle curve of the ground temperature process. During the winter period, the water temperature in a river is generally lower than the temperature of underground soil. Thus, the heat flux in the riverbed has a continuous influence on the temperature of water in a river. The heat flux between the water body under an ice cover and the riverbed at the bottom can be determined based on the Fourier law by the product of the heat transfer coefficient and the temperature gradient in soil (Jobson 1977). In practice, it is difficult to measure the temperature gradient in a riverbed medium. Therefore, it is normally assumed that the riverbed medium is a homogeneous material, the surface temperature of the riverbed medium is the same as the water temperature in contact with each other, and the insulation layer is 0.25 m below the surface of the riverbed. In this case, the change of the ground temperature is within 15% and a constant can be taken. According to the heat transfer principle of solid material, to simplify the calculation, the heat flux due to heat exchange between the riverbed medium and water is calculated by the following formula:

$$\phi_d = -k_d \frac{\partial T_d}{\partial z} \quad (10)$$

where  $\phi_d$  is the heat flux due to heat exchange between the underground soil and the water body in a river;  $k_d$  is the heat transfer coefficient between the water body and the riverbed medium;  $T_d$  is the ground temperature;  $z$  is the location selected

for calculating the heat flux, the origin of coordinates is located at the interface between the riverbed surface and water in a river, and the direction is perpendicular to the interface.

Based on data collected regarding the ground temperature of the IMRYR, the average ground temperature at the surface of the riverbed is about 5 °C, and that on the bank (under the water surface) is about 3 °C. Using the equivalent heat transfer coefficient and equivalent ground temperature method (Yang 2021), the equivalent heat flux between the riverbed and the water body can be determined using the following equations:

$$\phi_d^* = \frac{1}{\chi} \int_0^{\chi} \phi_d ds \approx \frac{1}{\chi} \chi_1 h_{d1} (T_w - T_{d1}) + \frac{1}{\chi} \chi_2 h_{d2} (T_w - T_{d2}) = h_d (T_w - T_d) \quad (11)$$

$$h_d = (\chi_1 h_{d1} + \chi_2 h_{d2}) / \chi \quad (12)$$

$$T_d = (\chi_1 h_{d1} T_{d1} + \chi_2 h_{d2} T_{d2}) / (\chi_1 h_{d1} + \chi_2 h_{d2}) \quad (13)$$

where  $\phi_d^*$  is the equivalent heat flux between the riverbed and the water body, W/m<sup>2</sup>;  $ds$  is the unit length of wetted perimeter of the riverbed;  $h_d$  is the equivalent heat transfer coefficient of the riverbed and the water body;  $T_d$  is the equivalent ground temperature of the riverbed; subscripts '1' and '2' represent the river bank slope and riverbed, respectively. For example,  $\chi_1$  is the partial wetted perimeter of river banks;  $\chi_2$  is the partial wetted perimeter of the riverbed.

Without considering ice production from the upstream section of the study river reach, assuming that all heat lost from the water body is used for ice production, the model for river ice production in the study river reach can be obtained based on the heat budget of the water body in the study river reach as,

$$\frac{dQ_i}{dt} = - \frac{\sum \phi^* A_s}{\rho_i L_i} \quad (14)$$

where  $Q_i$  is the amount of ice produced in the study river reach;  $t$  is the time;  $L_i$  is the latent heat of ice;  $\rho_i$  is the mass density of ice;  $A_s$  is the area for heat exchange and determined based on the measured data for the water surface area and river morphology.

#### 4. VARIATION OF ICE PRODUCTION

In the course of analysis of the variation of ice production and heat flux components, the daily heat flux calculated using the ice production model was denoted as  $\phi_e$ , the daily ice production was denoted as  $Q_e$ , and the difference between daily water temperature and air temperature was denoted as  $T_e$ . The total heat flux from the starting date to the  $n$ th day during an ice-covered period (termed as ' $n$ -day ice-covered period') is denoted as  $\phi_T$ , the total ice production is  $Q_T$ , and the accumulated value of the temperature difference between daily water temperature and air temperature is denoted as  $T$ . Thus, the following equations can be used to calculate these variables:

$$\phi_T = \sum_{i=1}^n \phi_e \quad (15)$$

$$Q_T = \sum_{i=1}^n Q_e \quad (16)$$

$$T = \sum_{i=1}^n T_e \quad (17)$$

##### 4.1. Variation of ice production with time

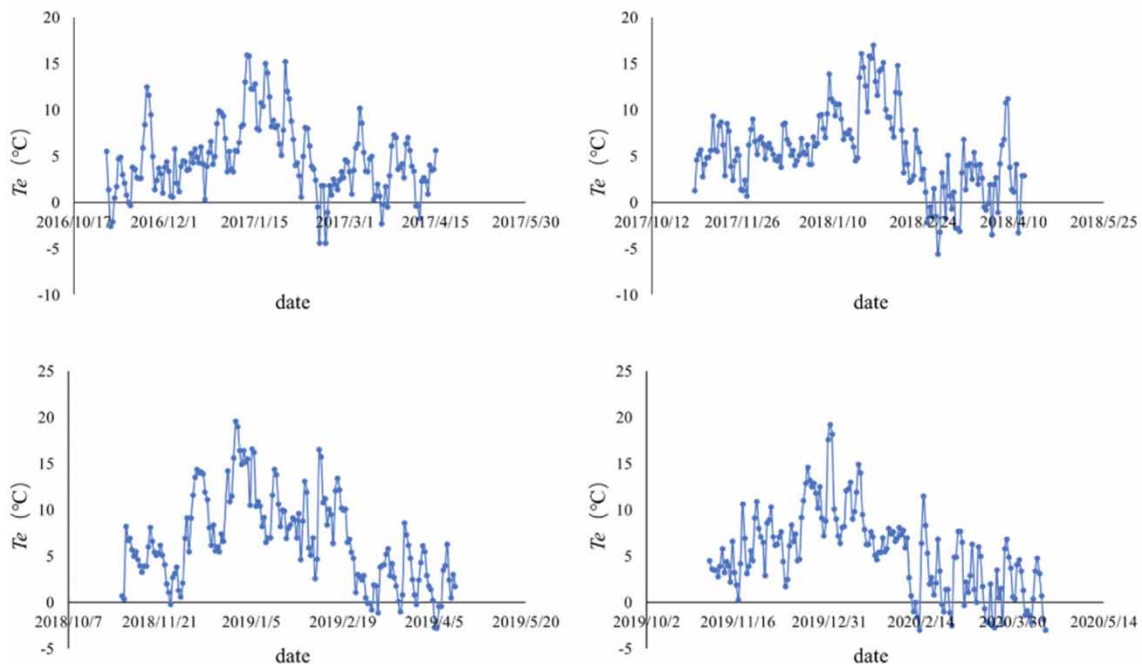
Based on hydrological and meteorological data during winter periods (from November 2 to April 15) from 2017 to 2020 collected at the Bayangaole gauging station, the characteristics of variation of the temperature difference between the daily water temperature and air temperature, heat flux, and ice production during winter in the Bayangaole station of the next year have been analyzed.

Figure 3 shows the variation of the difference between daily water temperature and air temperature at the Bayangaole station during the winter period from 2017 to 2020. One can see from Figure 3 the variation range of the temperature difference is large during the entire winter period. At the beginning of the winter period, the temperature difference is relatively small, about 5 °C. From December 10 to January 10 of the next year, the temperature difference increased significantly, and the peak temperature difference reached 20 °C. In February, the temperature difference became smaller and even became negative, since the air temperature starts to increase in February.

Figure 4 shows the change of the cumulative heat flux with the cumulative temperature difference (between water temperature and air temperature). One can see from Figure 4 that the cumulative heat flux clearly increases with the increase in the cumulative temperature difference.

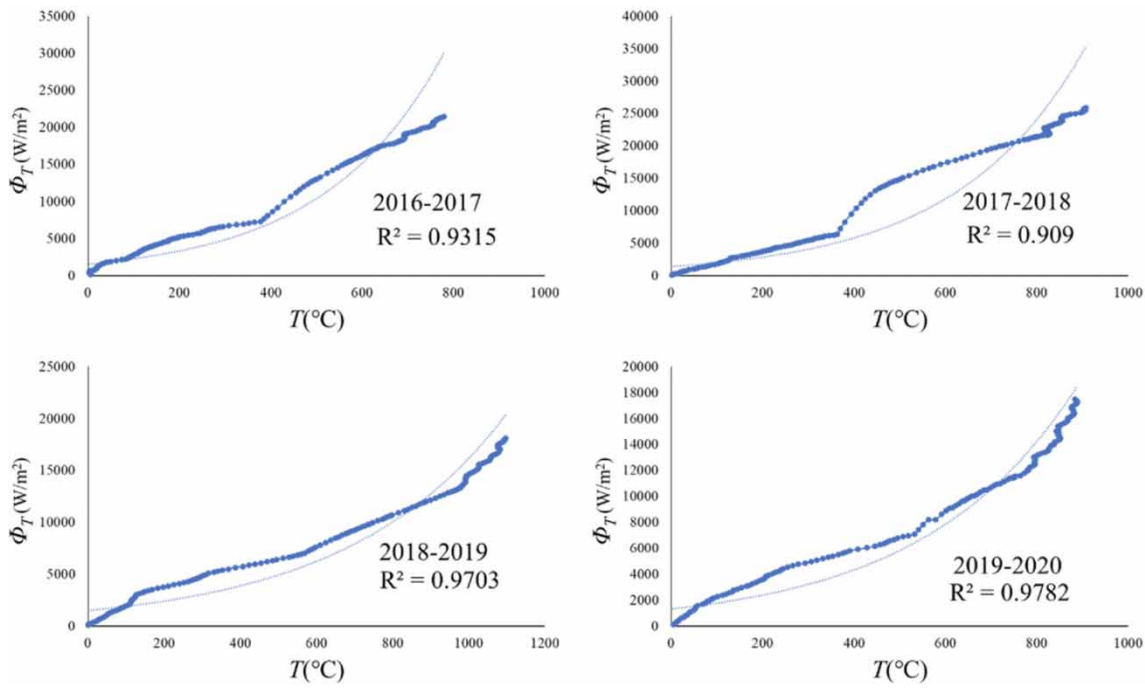
Figure 5 shows the variation of the daily heat flux during the winter of 2019/2020. Comparing to the variation of the temperature difference in Figure 3, one can see that the time of the sharp increase of the daily heat flux is similar to that of the temperature difference between the water temperature and air temperature, with a slight lag. The daily heat flux changes obviously during both river freeze-up and breakup periods. Results also show that the change of the heat flux during the river freeze-up period is much more than that during the break-up period. This is due to the bigger temperature difference between the water temperature and air temperature during the river freeze-up period comparing to that during the river break-up period. When an ice cover is formed in a river, the heat flux between the ice cover and the water body changes dramatically with the change of the flow velocity and the ice cover thickness. Thus, the heat flux between the atmosphere and the water body as well as between the riverbed and the water body also increases steadily with the decrease of air temperature. The influence of heat flux between the riverbed and the water body is relatively stable, and the magnitude is small during the ice-covered period, freeze-up, and break-up periods. Therefore, the heat flux from the atmosphere and ice cover on the water body is the main factor for determining the amount of ice production in rivers.

Figure 6 shows the daily ice production calculated by using the ice production model. The measured ice cover thickness change is also presented in Figure 6. At the beginning of the winter period, the daily ice production remains at a relatively stable value due to the continuous heat loss from the water body in the river. During this period, since the amount of ice produced in the study IMRYR is not enough to form an ice cover, frazil ice and ice pans produced in the river will be transported downstream. A sudden big drop of air temperature during the winter period results in a rapid increase in the production of frazil ice particles. These ice frazil ice particles collide with each other, and gradually form a lot of ice pans



**Figure 3** | Variations of the temperature difference between the daily water temperature and air temperature.





**Figure 4** | The cumulative change of the total heat flux with the temperature difference.

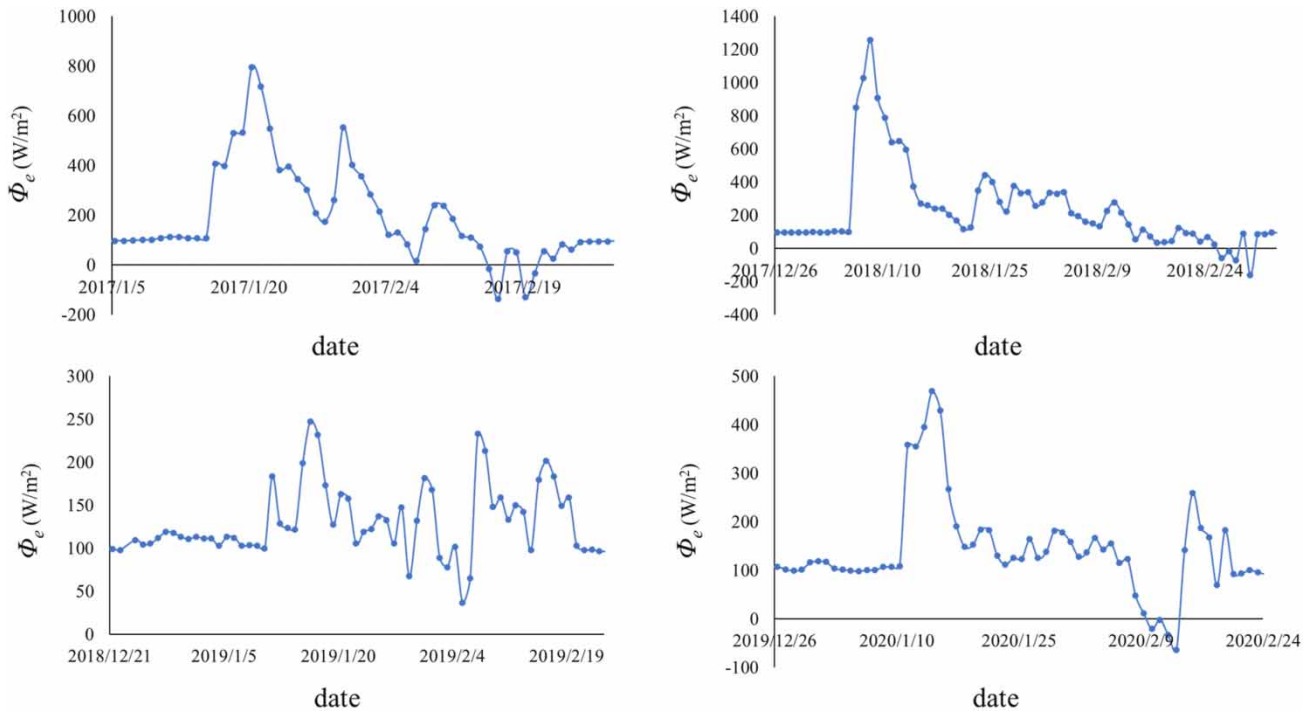


**Figure 5** | Variations of the daily heat flux.

floating on the water surface. When the area coverage of ice pans on the water surface increases, the ice transport capacity decreases. Ice pans collide with each other and slow down. With further increase in the amount of ice pans, ice pans become congested and jammed. Then, the formation of an initial ice cover will lead to a rapid development of an ice cover toward

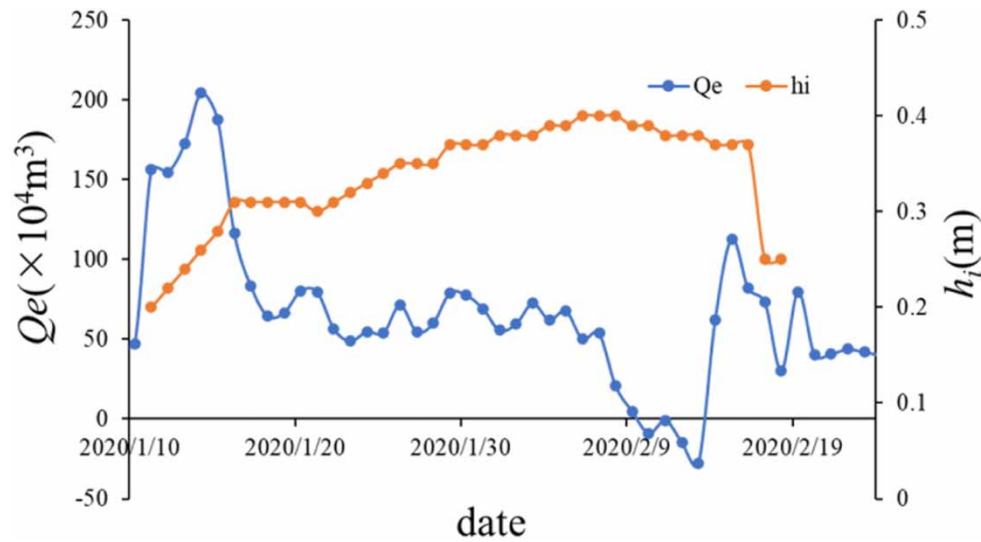


**Figure 6** | Daily ice production and ice cover thickness variation.

upstream, depending on the flow velocity and the incoming amount of ice pans on the water surface. In the meantime, the ice cover thickness increases accordingly. During the river freeze-up period, the daily ice production is normally higher than that in other periods since the water surface is not covered by ice, implying more heat exchange between the water body and air. During an ice-covered period, the thickening process of an ice cover continues. When the air temperature begins to rise, the daily ice production decreases, and the thickness of the ice cover gradually decreases until the period of river break-up. The variation trend of daily ice production was in good consistency with the variation of the ice cover thickness. Results of calculation showed that the temperature difference, heat flux, and ice production during the winter period of the other years are similar to those during the winter of 2019–2020.

The cumulative heat flux, total ice production, and cumulative temperature difference between water temperature and air temperature at the Bayangaole gauging station during each winter from 2017 to 2020 have been statistically analyzed. Results of the statistical analysis are shown in Table 1. Results indicated that when the total heat flux reaches  $7,388.58 \text{ W/m}^2$ , the total ice production reaches  $3.18 \times 10^7 \text{ m}^3$ , and the  $T$  value reaches  $472.92 \text{ }^\circ\text{C}$ , the Yellow River at the Bayangaole station will easily become ice-covered.

In order to assess the critical ice production for river freeze-up and break-up, the mean value of the daily heat flux before the period of river freeze-up ( $\phi_m$ ) has been calculated. Then, the difference between the daily heat flux and  $\phi_m$  has been calculated. Afterward, the effective ice production was further determined. Figure 7 shows the effective ice production at the Bayangaole gauging station during the winter of 2019–2020. By comparing Figure 7 to Figure 6, one can see that the effective ice production increases first and then decreases during the ice-covered period. When effective ice production is much higher than 0, the ice cover thickness begins to increase. When the effective ice production is much less than 0, the ice cover thickness begins to decrease. When the effective ice production is about 0, the ice cover thickness basically keeps unchanged, and no new ice cover will be developed.

**Table 1** | River freeze-up date and total ice production at the Bayangaole station during the winter period

Year	2016–2017	2017–2018	2018–2019	2019–2020	Average value
Freeze-up date	2017/1/16	2018/1/6	2019/1/11	2020/1/11	
$\phi_T$ ( $\text{W/m}^2$ )	7,683.08	7,201.77	7,222.64	7,446.83	7,388.58
$Q_T$ ( $10^7 \text{ m}^3$ )	3.175	3.143	3.152	3.250	3.180
$T$ ( $^\circ\text{C}$ )	402.40	370.20	577.70	541.40	472.92

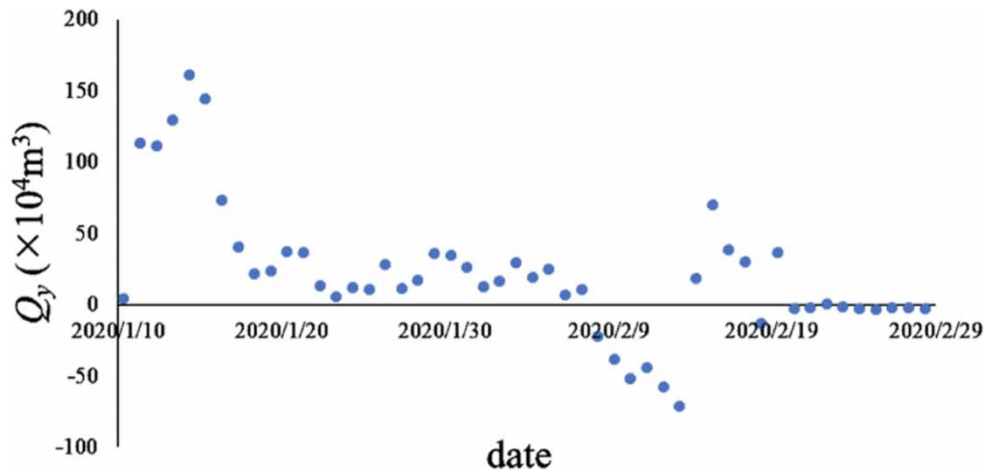


**Figure 7** | Changes of effective daily ice production at the Bayangaole station during the winter of 2019–2020.

#### 4.2. Ice production at different locations

Table 2 shows calculation results of ice production at the following four gauging stations along the IMRYR during winter periods from 2016 to 2020: Bayangaole, Sanhuhekou, Baotou, and Toudaoguai gauging stations (note: each winter period starts from 2 November to 15 April of next year). As shown in the table, the highest annual ice production occurred at the Bayangaole station and the lowest annual ice production happened at the Toudaoguai station. Clearly, the average annual ice production decreased from the upstream Bayangaole station to the downstream Toudaoguai station of the IMRYR.

The total ice production depends not only on the heat flux but also on the area size for heat transfer. The variation of the daily heat flux in each river section directly reflects the amount of ice production per unit area. To simplify the calculation by using the ice production model, in each channel section, the areas for heat transfer at the water surface and the riverbed are assumed as unchanged. In the following, the calculation is presented by taking the winter of 2017–2018 as an example, since the total ice production at Bayangaole, Sanhuhekou, Baotou, and Toudaoguai gauging stations reaches the maximum value. Figure 8 describes the daily heat flux in the winter of 2017–2018. The peak value of the daily heat flux at the Bayangaole station appeared later than that at the other three stations, indicating that the river freeze-up at the Bayangaole station was later than that at the other three places. The measured data showed that the river freeze-up at the Bayangaole station occurred on 1 January 2018. The peak value of heat flux appeared first at the Toudaoguai station, and the observed data showed that the date for river freeze-up at the Toudaoguai station occurred on 8 November 2017, earlier than the other three places. The peak value of heat flux was the largest at the Bayangaole station and the smallest at the Sanhuhekou station. Before and after 1 March, the daily heat flux appeared negative successively. At this time, the process of ice production in the river stopped, and the melting process occurred along the river reach.

The relationship between the cumulative temperature difference (between water temperature and air temperature) during the winter of 2017–2018 and the total heat flux is shown in Figure 9. During the winter period of 2017–2018, the total heat flux increased with the increase of the cumulative temperature difference, with the highest heat flux at the Toudaoguai station,

**Table 2** | Results of the statistical analysis of total ice production during winter ( $10^7 \text{ m}^3$ )

Station	Winter period				Average
	2016–2017	2017–2018	2018–2019	2019–2020	
Bayangaole	9.336	11.280	7.902	7.624	9.036
Sanhuhekou	5.187	5.311	6.029	5.192	5.430
Baotou	2.290	5.079	4.093	3.659	3.780
Toudaoguai	2.402	4.431	2.875	2.223	2.983

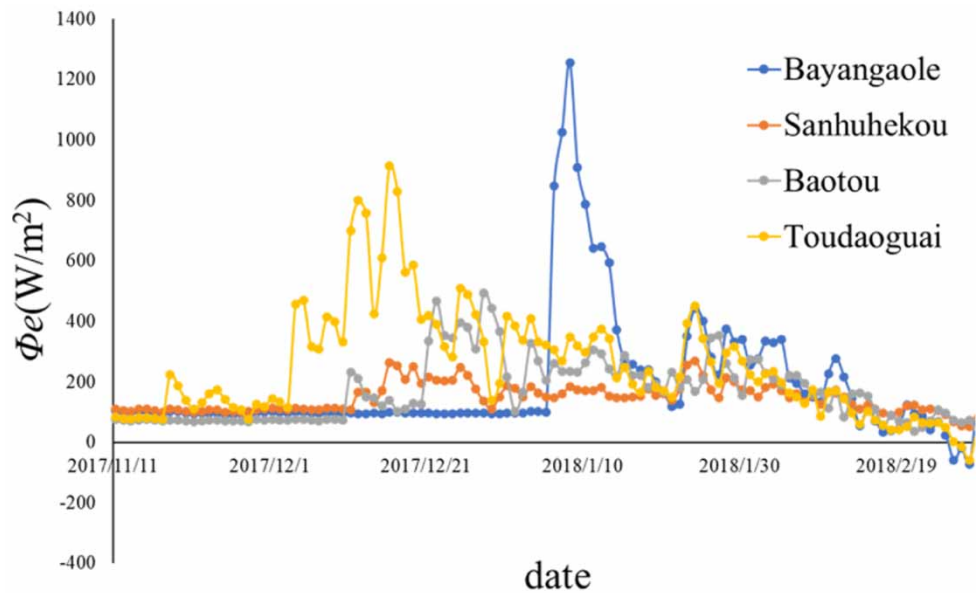


**Figure 8** | Daily heat flux during the winter of 2017–2018 at different stations.

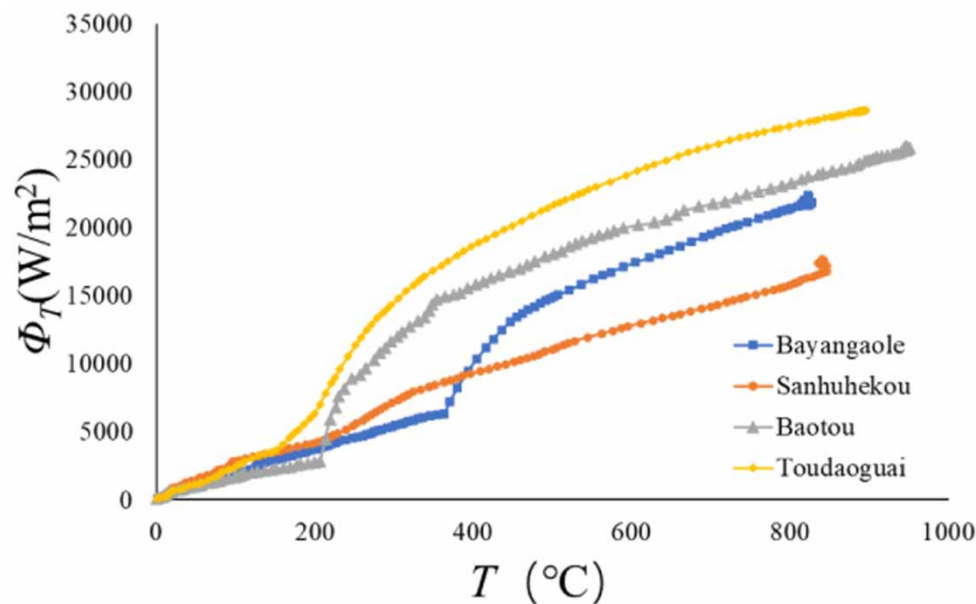


**Figure 9** | Relationship between the cumulative temperature difference and the total heat flux during the winter of 2017–2018.

followed by Baotou and Bayangaole, and the lowest in the Sanhuhekou stations. Both Figures 4 and 9 show the same dependency of the total heat flux on the cumulative temperature difference.

#### 4.3. Sensitivity analysis

The key factors affecting ice production are thermal factor and hydraulic factor, including the air temperature, radiation, flow discharge, and water surface area. The air temperature, radiation intensity, and flux change affect the magnitude of heat flux. The water surface area not only affects the heat flux, but also affects the amount of ice production. Based on the values of

**Table 3** | Sensitivity analysis of variables in the ice production model

	Variable	Original value	Adjusted value	Difference (%)	Test results (10 <sup>7</sup> m <sup>3</sup> )	Change in results (%)
Test 0	/	/	/	0	4.920	0
Test 1	Air temperature (°C)	-15.9	-12.72	+20	4.689	-4.69
Test 2	Air temperature (°C)	-15.9	-19.08	-20	5.168	5.05
Test 3	Discharge (m <sup>3</sup> /s)	573	687.6	+20	4.768	-3.09
Test 4	Discharge (m <sup>3</sup> /s)	573	458.4	-20	4.768	3.09
Test 5	Radiation (W/m <sup>2</sup> )	180.99	217.18	+20	5.146	-2.29
Test 6	Radiation (W/m <sup>2</sup> )	180.99	151.19	-20	4.807	4.59
Test 7	Surface area (m <sup>2</sup> )	500	600	+20	5.382	9.39
Test 8	Surface area	500	400	-20	4.355	-11.48

primary variables in the ice production model, only one variable value is adjusted each time to assess the change of calculation results, and then to analyze the influence of each factor on the calculation results by using the ice production model.

Through the analysis of measured data, the variation range of variables is within 20%, and the changed variables are still in line with the actual situation of natural rivers. In order to clearly compare the influence of various variables on the calculation results, the variation range of sensitivity analysis is selected as 20% in consideration of the actual situation of measured data of the Yellow River. Considering the characteristics of each variable in the ice production model, the following adjustments on each influencing variable have been made based on the actual situation of the IMRYR, as shown in Table 3. One can see from Table 3, with the same amount of adjustment in percentage for each variable, the change (in percentage) of the final testing result is different. Results showed that the influence degree of each variable on the ice production was in a descending order as follows: water surface area, air temperature, radiation, and discharge. Comparing to the variation range of the calculated ice production, the ice production model is sensitive to the variation of the water surface area and air temperature. Particularly, when the value of the water surface area is adjusted by 20%, 11.48% of the final calculated result of ice production will be affected. Thus, the accurate measurement of the water surface area is very important for determining the ice production in a river.

## 5. CONCLUSIONS

To calculate the ice production in a natural river, the heat flux between the ice cover and the water body and between the riverbed and water must be considered. The Colburn analogy method is coupled with the heat transfer principle of solid plate and the thermodynamic model. Based on this method, the ice production model has been established. The variation trend of the daily ice production was consistent with that of the ice cover thickness. Results of analysis during river freeze-up periods from 2017 to 2020 showed that when the total ice production in the Bayangaole gauging station reaches  $3.18 \times 10^7 \text{ m}^3$ , river freeze-up is likely to occur.

The characteristics of ice production in the IMRYR indicate that the daily heat flux is closely related to the river freeze-up and ice cover thickness. The effective ice production has been determined based on the difference between the daily heat flux and the mean value of the daily heat flux before the period of river freeze-up. When effective ice production is much higher than 0, the ice cover thickness begins to increase. When the effective ice production is much less than 0, the ice cover thickness begins to decrease. When the effective ice production is about 0, the ice cover thickness basically keeps unchanged, and no new ice cover will be developed. Results showed that the highest annual ice production occurred at the Bayangaole station, and the lowest annual ice production happened at the Toudaoguai station. Clearly, the average annual ice production decreased from the upstream Bayangaole station to the downstream Toudaoguai station of the IMRYR. The cumulative temperature difference between the water temperature and air temperature has a strong correlation with the total heat flux. The sensitivity analysis of the variables in the ice production model and ice production has been carried out. The degree of influence of each variable on the ice production was in the following order: water surface area, air temperature, radiation, and discharge.

The present study has been carried out based on the limited field data collected from four gauging stations. Only the heat flux along the study river reach has been considered. The ice production from the upstream section of the study river reach has not been considered. Clearly, long-term systematic observations along the entire IMRYR during the ice-covered period should be conducted to obtain more comprehensive field data for further improving the accuracy of the model for ice production.

## ACKNOWLEDGEMENT

This research is supported by the National Natural Science Foundation of China (Grant Numbers: 51879065 and U2243221). The authors are grateful for the financial support.

## DATA AVAILABILITY STATEMENT

All relevant data are included in the paper or its Supplementary Information.

## CONFLICT OF INTEREST

The authors declare there is no conflict.

## REFERENCES

- Ashton, G. D. 1985 [Deterioration of floating ice covers](#). *Journal of Energy Resources Technology* **107** (2), 177–182.
- Ashton, G. D. 1986 *River and Lake Ice Engineering*. Water Resources Publications, Littleton, Colorado, 80161, USA.
- Benson, B. J., Magnuson, J. J., Jensen, O. P., Card, V. M., Hodgkins, G., Korhonen, J., Livingstone, D. M., Stewart, K. M., Weyhenmeyer, G. A. & Granin, N. G. 2012 [Extreme events, trends, and variability in Northern Hemisphere lake-ice phenology \(1855–2005\)](#). *Climatic Change* **112** (2), 299–323.
- Bull, G. A. 1920 Smithsonian meteorological tables. Smithsonian meteorological tables. *Nature* **106** (2657), 142–143.
- Cheng, Z. A., Pang, X. P., Zhao, X. & Tan, C. 2017 [Spatio-temporal variability and model parameter sensitivity analysis of ice production in ross ice shelf polynya from 2003 to 2015](#). *Remote Sensing* **9**, 934.
- Comiso, J. C., Kwok, R., Martin, S. & Gordon, A. L. 2011 Variability and trends in sea ice extent and ice production in the Ross Sea. *Journal of Geophysical Research Oceans* **116**, C04021.
- Freysteinson, S. 1970 Calculation of Frazil Ice Production. Proceedings of the Symposium on Ice and Its Action on Hydraulic Structures, International Association for Hydraulics Research, Reykjavik, Iceland, 12 pp.
- Jobson, H. E. 1977 [Bed conduction computation for thermal models](#). *Journal of the Hydraulics Division* **103** (HY10), 1213–1217.
- Launiainen, J. & Cheng, B. 1998 [Modelling of ice thermodynamics in natural water bodies](#). *Cold Regions Science & Technology* **27** (98), 153–178.
- Lees, K., Clark, S. P., Malenchak, J. & Chanel, P. 2021 [Characterizing ice cover formation during freeze-up on the regulated Upper Nelson River](#). *Manitoba. Journal of Cold Regions Engineering* **35** (3), 04021009.
- Li, N., Tuo, Y. C., Deng, Y., Li, J., Liang, R. F. & An, R. D. 2016 [Heat transfer at ice-water interface under conditions of low flow velocities](#). *Journal of Hydrodynamics* **28** (04), 603–609.
- Mao, Z. Y. & Chen, C. Z. 1999 Simulation of heat transfer between streambed and river flow. *Water Resources and Hydropower Engineering* **30** (5), 11–13. (in Chinese).
- Marsh, P. & Prowse, T. D. 1987 [Water temperature and heat flux at the base of river ice covers](#). *Cold Regions Ence & Technology* **14** (1), 33–50.
- Maykut, G. A. 1982 [Large-scale heat exchange and ice production in the central Arctic](#). *Journal of Geophysical Research: Oceans* **87**, 7971–7984.
- Maykut, G. A. & Untersteiner, N. 1971 [Some results from a time dependent thermodynamic model of sea-ice](#). *Journal of Geophysical Research* **76** (6), 1550–1575.
- Paily, P. P., Macagno, E. O. & Kennedy, J. F. 1974 Winter-regime surface heat loss from heated streams. *journal of the Hydraulics division* **75**, 7347005.
- Sarraf, S. & Zhang, X. T. 1996 [Modeling ice-cover melting using a variable heat transfer coefficient](#). *Journal of Engineering Mechanics* **122** (10), 930–938.
- Shen, H. T. & Chang, L. A. 1984 [Simulation of growth and decay of river ice cover](#). *Journal of Hydraulic Engineering* **110** (7), 958–971. (in Chinese).
- Shen, H. T. & Ruggles, R. W. 2010 [Winter heat budget and frazil ice production in the upper st.lawrence river](#). *Journal of the American Water Resources Association* **18** (2), 251–256.
- Smits, A. P., Gomez, N. W., Dozier, J. & Sadro, S. 2021 Winter climate and lake morphology control ice phenology and under-ice temperature and oxygen regimes in mountain lakes. *Journal of Geophysical Research: Biogeosciences* **126** (8), G006277.

- Sui, J., Wang, D. & Karney, B. 2000 Sediment concentration and deformation of riverbed in a frazil jammed river reach. *Canadian Journal of Civil Engineering* **27** (6), 1120–1129.
- Sui, J., Karney, B., Sun, Z. & Wang, D. 2002 Field investigation of frazil jam evolution – a case study. *ASCE Journal of Hydraulic Engineering* **128**, 781–787.
- Sui, J., Karney, B. & Fang, D. 2005 Variation in water level under ice-jammed condition – field investigation and experimental study. *Hydrology Research* **36** (1), 65–84.
- Sui, J., Hicks, F. & Menounos, B. 2006 Observations of riverbed scour under a developing hanging ice dam. *Canadian Journal of Civil Engineering* **33** (2), 214–218.
- Sui, J., Thring, R., Karney, B. & Wang, J. 2007 Effects of river ice on stage-discharge relationships – a case study of the Yellow River. *International Journal of Sediment Research* **22** (4), 263–272.
- Sui, J., Wang, J., Balachandar, R., Sun, Z. & Wang, D. 2008 Accumulation of frazil ice along a river bend. *Canadian Journal of Civil Engineering* **35**, 158–169.
- Tuo, Y. C. 2018 Effects of dam reconstruction on thermal-ice regime of Fengman Reservoir. *Cold Regions Science and Technology* **146**, 223–235.
- Untersteiner, N. 1964 Calculations of temperature regime and heat budget of sea-ice in the central Arctic. *Journal of Geophysical Research* **69** (22), 4755–4766.
- Wang, J., Fu, H., Yin, K. M., Yin, Y. J. & Gao, Y. X. 2007 Analysis of stages under ice-covered in winter. *Advances in Water Science* **1**, 102–107. (in Chinese).
- Wang, J., Hou, Z. X., Sun, H. J., Fang, B. H., Sui, J. & Karney, B. 2021 Local scour around a bridge pier under ice-jammed flow condition -an experimental study. *Journal of Hydrology and Hydromechanics* **69** (3), 275–287.
- Yang, K. L. 2021 Heat exchange model between river-lake and atmosphere during ice age. *Journal of Hydraulic Engineering* **52** (5), 556–564, 577. (in Chinese).
- Zhao, S. X., Shen, H. T., Shi, X. H., Li, C. Y., Li, C. & Zhao, S. N. 2020 Wintertime surface heat exchange for the inner Mongolia reach of the Yellow River. *JAWRA Journal of the American Water Resources Association* **56** (2), 348–356.

First received 14 May 2022; accepted in revised form 12 August 2022. Available online 30 August 2022